

Materials Technology

Advanced Performance Materials

ISSN: 1066-7857 (Print) 1753-5557 (Online) Journal homepage: <http://www.tandfonline.com/loi/ymte20>

Bioactive conformable hydrogel-carbonated hydroxyapatite nanocomposite coatings on Ti-6Al-4V substrates

Kyung-Ah Kwon, Judith A. Juhasz, Roger A. Brooks & Serena M. Best

To cite this article: Kyung-Ah Kwon, Judith A. Juhasz, Roger A. Brooks & Serena M. Best (2018): Bioactive conformable hydrogel-carbonated hydroxyapatite nanocomposite coatings on Ti-6Al-4V substrates, *Materials Technology*, DOI: [10.1080/10667857.2018.1475143](https://doi.org/10.1080/10667857.2018.1475143)

To link to this article: <https://doi.org/10.1080/10667857.2018.1475143>



© 2018 The Author(s). Published by Informa UK Limited, trading as Taylor & Francis Group.



Published online: 14 Jun 2018.



Submit your article to this journal [↗](#)



Article views: 33



View Crossmark data [↗](#)

Bioactive conformable hydrogel-carbonated hydroxyapatite nanocomposite coatings on Ti-6Al-4V substrates

Kyung-Ah Kwon^a, Judith A. Juhasz^a, Roger A. Brooks^b and Serena M. Best^a

^aDepartment of Materials Science and Metallurgy, Cambridge Centre for Medical Materials, University of Cambridge, Cambridge, United Kingdom; ^bDivision of Trauma & Orthopaedic Surgery, University of Cambridge, Cambridge, United Kingdom

ABSTRACT

A series of nanocomposite coatings was produced, comprising a hydrogel polymer, poly(2-hydroxyethyl methacrylate)/poly(ϵ -caprolactone) (PHEMA/PCL) matrix with nanoscale carbonated hydroxyapatite (nCHA) filler particles. The weight fraction of the filler was varied from 0 to 20% and the composites were applied as coatings onto Ti-6Al-4V substrates. The filler distribution and surface morphology were investigated by AFM, and the mechanical stability of the coatings was characterised using nanoindentation in both dry and wet conditions. The cellular response to the coatings was also examined *in vitro* using human osteoblast (HOB) cells. It was found that interfacial cracking occurred for composites containing greater than 10 wt.% nCHA and that 10 wt.% nCHA composite coatings appear to offer the greatest coating stability and bioactivity compared with the other composite coatings. It was concluded that the nCHA-containing PHEMA/PCL composite coatings had the potential to provide a soft, low modulus interface between metal implants and bone.

ARTICLE HISTORY

Received 14 March 2018
Accepted 4 May 2018

KEYWORDS

Hydrogel; carbonated hydroxyapatite; nanocomposite; coating; Ti-6Al-4V

Introduction

Titanium (Ti) or titanium alloys including Ti-6Al-4V have been used successfully as dental and orthopaedic implants for decades [1]. There has also been considerable interest in producing coated implants to promote enhanced bioactivity at the bone implant and interface [2]. However, many commercially available coatings are brittle in nature and unable to conform to the surface topography of the osseous environment into which they are placed.

Hydroxyapatite (HA) is a bioactive and osteoconductive material, which has similar phase composition and crystal structure to natural bone mineral. It has the formula, $\text{Ca}_{10}(\text{PO}_4)_6(\text{OH})_2$ and is one of a family of calcium phosphate compounds which have been used in orthopaedic implants. Apart from calcium and phosphorus ions in natural bone mineral carbonate ion (CO_3^{2-}) has been found to be the most abundant ion, occupying 2–8 wt.% of the inorganic component of bone [3]. This makes the carbonated hydroxyapatite (CHA) have a more similar chemical composition to the natural bone mineral than HA. Not only does CHA have greater osteoconductivity than HA [4,5] but it is also bioresorbable [6].

HA coatings on metal implants have been reported to create an osteophilic surface that will accelerate bone formation in the initial stages of osseointegration, resulting in chemical fixation of the implant to bone, thereby

enhancing the stability and reducing the movement of the implant. However, these HA coatings do not overcome the potential issues of stress shielding and for this, a low modulus coating might be desirable. The use of a hydrogel, in particular crosslinked poly(2-hydroxyethyl methacrylate) (PHEMA), as an interfacial coating material between a metallic implant and bone has been investigated by Netti *et al.* [7] with the view that the swelling capacity of the PHEMA in a constrained environment would offer a mechanism to fix a metallic implant in an intramedullary cavity. Pull-out test *in vitro* and an *in vivo* study using PHEMA-coated Ti pins implanted in the diaphysis of rabbits showed promising results.

This study aims to produce and characterise bioactive coatings that are conformable when wet, and resorbable once the bone repair process has occurred. The addition of polycaprolactone (PCL) into PHEMA hydrogel was reported to improve both mechanical strength and cell activity [8], suggesting that this might be a good option for the matrix component of a composite. Nano-sized particles incorporated into composites have been reported to alter the potential for more uniform filler distribution with improved mechanical and physical properties than microcomposites [9–11]. Therefore, a series of PHEMA/PCL-nCHA nanocomposites was prepared and applied to coat Ti-6Al-4V substrates followed by investigation of their physical, mechanical and biological properties.

Materials and methods

Production and characterisation of nCHA

Nano-sized CHA particles were produced using the aqueous precipitation method proposed by Gibson and Bonfield [12]. Briefly, carbonate ions were produced by bubbling CO₂ gas into deionised water (DIW) and 7.5 mM orthophosphoric acid (H₃PO₄, 85%, VWR) was added into this 'carbonated DIW'. nCHA was synthesised by adding this mixture to 13.2 mM calcium hydroxide (Ca(OH)₂, VWR) at 5 ml/min. Once addition was complete, the mixture was stirred for 2 hours and left overnight at room temperature to age. After aging, the resulting precipitates were filtered using a vacuum pump and subsequently dried at 80°C for 24 hours prior to characterisation.

The phase composition of nCHA was determined by X-ray diffractometry (XRD: Philips Gen4 PW3719) with CuKα radiation. XRD was operated at 40 mA and 40 kV, analysing nCHA between 2θ range of 18–42° with a step of 0.05° and a dwell time of 2 seconds. Fourier transform infrared spectroscopy (FTIR, Bruker Optics Tensor 27) was used to characterise the chemical composition. Data were collected over the wavenumber range of 700–4000 cm⁻¹ at a resolution of 4 cm⁻¹. The carbon elemental analyser was used to determine the carbonate ion content in nCHA by measuring the amount of CO₂ gas produced when nCHA was heated. Transmission electron microscopy (TEM: JEOL 2000FX) was used to observe the morphology of nCHA at an operated voltage of 200 kV.

Production of hydrogel-nCHA composite coatings

The coating substrates were prepared by cutting 10 mm diameter rods of Ti-6Al-4V (Advanced Titanium Metals Ltd, UK) into discs of 2 mm thickness. After the cutting, each disc was ultrasonically cleaned with ethanol for 30 minutes followed by rinsing with DIW and air-drying. The cleaned discs were etched using hydrochloric acid (HCl, 38%, Fisher Scientific) at 40°C for 3.5 hours followed by ultrasonic cleaning in acetone for 30 minutes. They were then rinsed thoroughly with DIW and air-dried.

The composite coating materials were prepared by first melting pellets of polycaprolactone (PCL, Aldrich) in 2-hydroxyethyl methacrylate (HEMA, 97% Aldrich) at 60°C at a weight ratio of 1:4, respectively. When PCL was completely dissolved, the following chemicals were added and mixed for 2 hours: 0.5 wt.% of benzoyl peroxide (BPO, 70%, Aldrich) and ethylene glycol dimethacrylate (EGDMA, 98%, Aldrich) based on the weight of HEMA as the initiator and the crosslinking agent, respectively. Varying weight fractions (0–20 wt.%) of the filtered, still wet,

nCHA precipitates was also added based on the weight of the total composite sample. The composite coatings on Ti-6Al-4V substrates were produced by a moulding technique followed by curing at 80°C in an oven.

Characterisation of hydrogel-nCHA composite coatings

Atomic force microscopy (AFM)

AFM was used to investigate both the coating surface morphology and the filler distribution. AFM in tapping mode was performed both in ambient and wet conditions using a Veeco Nanoscope V (Digital Instruments, Veeco Metrology Group). For both conditions, 10 μm × 10 μm areas of the coating surfaces were scanned and topographic (height) images were taken. For ambient AFM, phase images were also taken simultaneously. The two-representative composite coating samples with the lowest (0 wt.%) and highest (10 wt.%) filler contents were chosen to investigate in wet conditions. Prior to wet AFM, each sample was hydrated in deionised water (DIW) at 37°C for 3 days and the sample remained fully submerged in DIW throughout the test.

Nanoindentation

An MTS nanoindenter XP (MTS Nanoinstruments) was used to investigate the modulus of the composite-coated samples both in dry and wet conditions. Prior to wet tests, each sample was pre-soaked in DIW at 37°C for 3 days and it was made sure to be completely submerged in DIW throughout the test.

A spherical sapphire tip of 500 μm radius was used and a loading-unloading cycle was applied with a hold period of 10 seconds at the maximum load in order to dissipate creep deformation prior to unloading. During each test, a load-displacement curve was recorded and the modulus (E) was calculated by Equation 1.

$$h^{3/2} = \frac{3}{4\sqrt{R}} P \frac{(1 - \nu^2)}{E} \quad (\text{Eq.1})$$

where P and h are load and displacement respectively, ν is Poisson's ratio, and R is the spherical indenter tip radius [13].

Human osteoblast (HOB) cell culture study

The cellular response to composite coatings was investigated using primary human osteoblast cells (HOBs) obtained from enzymatic digestion of trabecular bone from femoral heads donated by total hip replacement patients following the guidelines for local ethical committee approval (LREC No. 06/Q0108/213) and informed consent (Addenbrooke's Hospital, Cambridge). All the samples were pre-soaked in

culture medium (McCoy's 5A solution without phenol red (BioConcept, Switzerland) supplemented with 10% foetal bovine serum, 1% penicillin-streptomycin-glutamine and 25 $\mu\text{g}/\text{ml}$ vitamin C) for 3 days at 37°C in a humidified atmosphere of 95% air and 5% CO_2 before seeding HOBs at a concentration of 2×10^4 cells/ cm^2 . After seeding, the samples were incubated for 4 hours to allow the cells to attach to the surface and then transferred to 24-well culture plates (using only the central eight wells). A volume of 1 ml of culture medium was added to each well and the samples were further incubated for up to 14 days. In order to improve coating adhesion of the nCHA-free composite, Ti-6Al-4V discs were mechanically ground rather than HCl-etched.

Scanning electron microscopy with energy dispersive spectroscopy (SEM-EDS) was used to observe the morphology of HOBs growing on each different composite coating at days 3 and 14 by taking each sample out from culture medium and rinsing with 0.9% NaCl solution. After the rinse, the cells were fixed in 4% glutaraldehyde in HEPES (4-(2-hydroxyethyl)-1-piperazineethanesulphonic acid) buffer solution (Sigma Aldrich, UK). All the cell-fixed samples were critical-point dried and then sputter coated with palladium for 90 seconds. For imaging, a secondary electron mode was used at an accelerating voltage of 15 kV.

Results

Carbonated hydroxyapatite nanoparticles (nCHA)

The XRD pattern of CHA matched well with the result expected for phase-pure synthetic HA (Figure 1(a)). All expected major peaks, such as (002), (211), and (300), were present in the XRD pattern. The vibrations associated with phosphate, hydroxyl and carbonate peaks were also identified on the FTIR spectrum (Figure 1(b)): peaks at 964, 1022, and 1092 cm^{-1} for phosphate group, peak at 3572 cm^{-1} for hydroxyl group and peaks at 872, 1420, 1447, 1539, and 1558 cm^{-1} for carbonate group. The carbon elemental analysis revealed that the CHA produced contained 3.90 ± 0.21 wt.% carbonate.

TEM micrograph is shown in Figure 1(c), and indicates that each particle had a needle-like morphology with approximate dimensions of 80–120 nm in length and 20–40 nm in width.

PHEMA/PCL-nCHA composite coatings on Ti-6Al-4V

Figure 2 shows the composite coatings on Ti-6Al-4V discs at a range of nCHA loadings. Those containing 0–10 wt.% nCHA show homogeneous and smooth composite coatings (Figure 2(a-c)) whilst those with 12–20 wt.% nCHA show coating cracking failures (Figure 2(d-f)).

Figure 3 shows the height and corresponding phase images of composite coatings scanned by AFM under ambient conditions. While the surface appeared relatively flat and smooth for the nCHA-free sample, it looked rough for the filled samples. The bright regions in the phase images of nCHA-filled composite coatings were found to be populated by particles of size ranging from 50 to 100 nm, the 10 wt.% nCHA-filled composite coating showing more bright regions than the 5 wt.% nCHA-filled composite coating. No such nano-particles could be observed in the phase image of the filler-free sample (Figure 3(b)). Immersing 10 wt.% nCHA-filled composite coating in DIW for 3 days significantly changed the surface feature while no such significant difference was observed for the filler-free composite coating. The globule-aggregates observed in the dry height image (Figure 3(f)) were no longer visible on the hydrated height image.

Throughout all the nanoindentation tests, neither coating delamination nor coating cracking were observed. Figure 4 shows the load-displacement curves of composite coatings tested both in dry and wet conditions (Figure 4(a-b)). The modulus of the coatings calculated is also shown in Figure 4(c-d). In dry conditions, increasing the nCHA content increased the modulus of the composite coating in a near linear fashion from 127 MPa for 0 wt.% nCHA-containing sample to 736 MPa for 10 wt.% nCHA-containing sample (Figure 4(c)). Although no similar

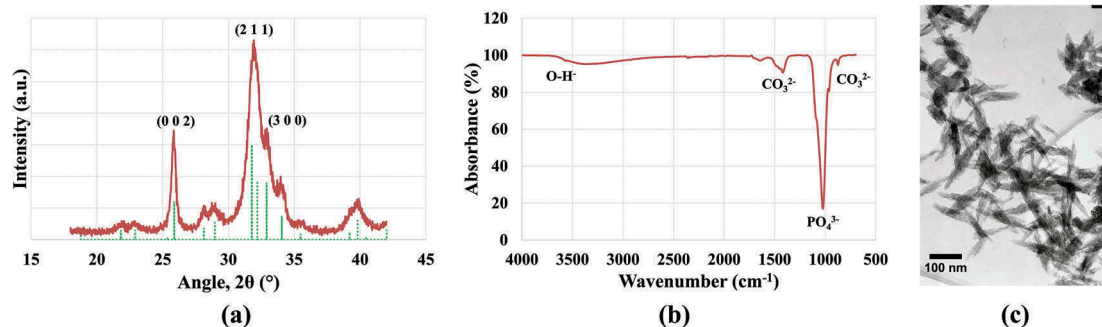


Figure 1. (a) XRD pattern (solid line) of carbonated hydroxyapatite (CHA) with XRD peaks of synthetic HA (ICDD: 09–0432, dotted line) (b) FTIR spectrum and (c) TEM image of CHA synthesised.

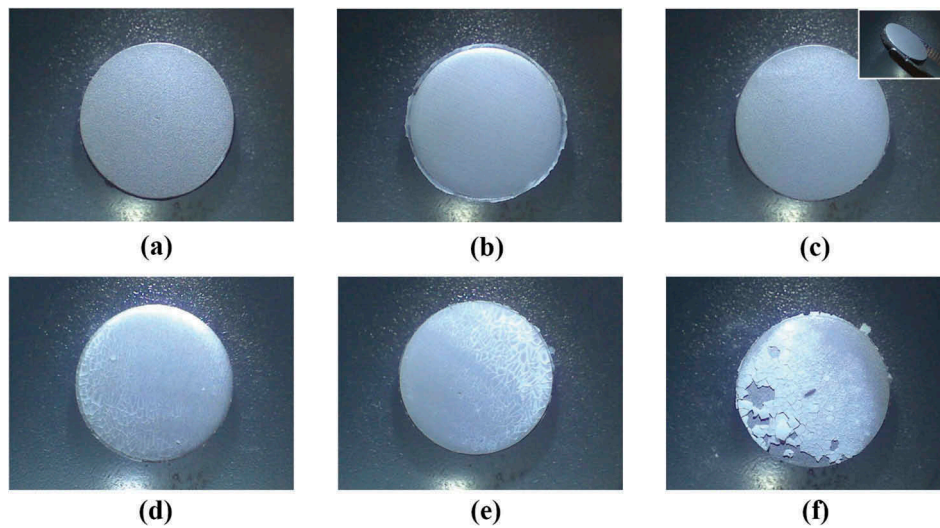


Figure 2. PHEMA/PCL-nCHA composite coatings onto Ti-6Al-4V discs (a) 0 wt.% nCHA (b) 5 wt.% nCHA (c) 10 wt.% nCHA; the inset depicting the same composition coating in a tilt view (d) 12 wt.% nCHA (e) 15 wt.% nCHA (f) 20 wt.% nCHA.

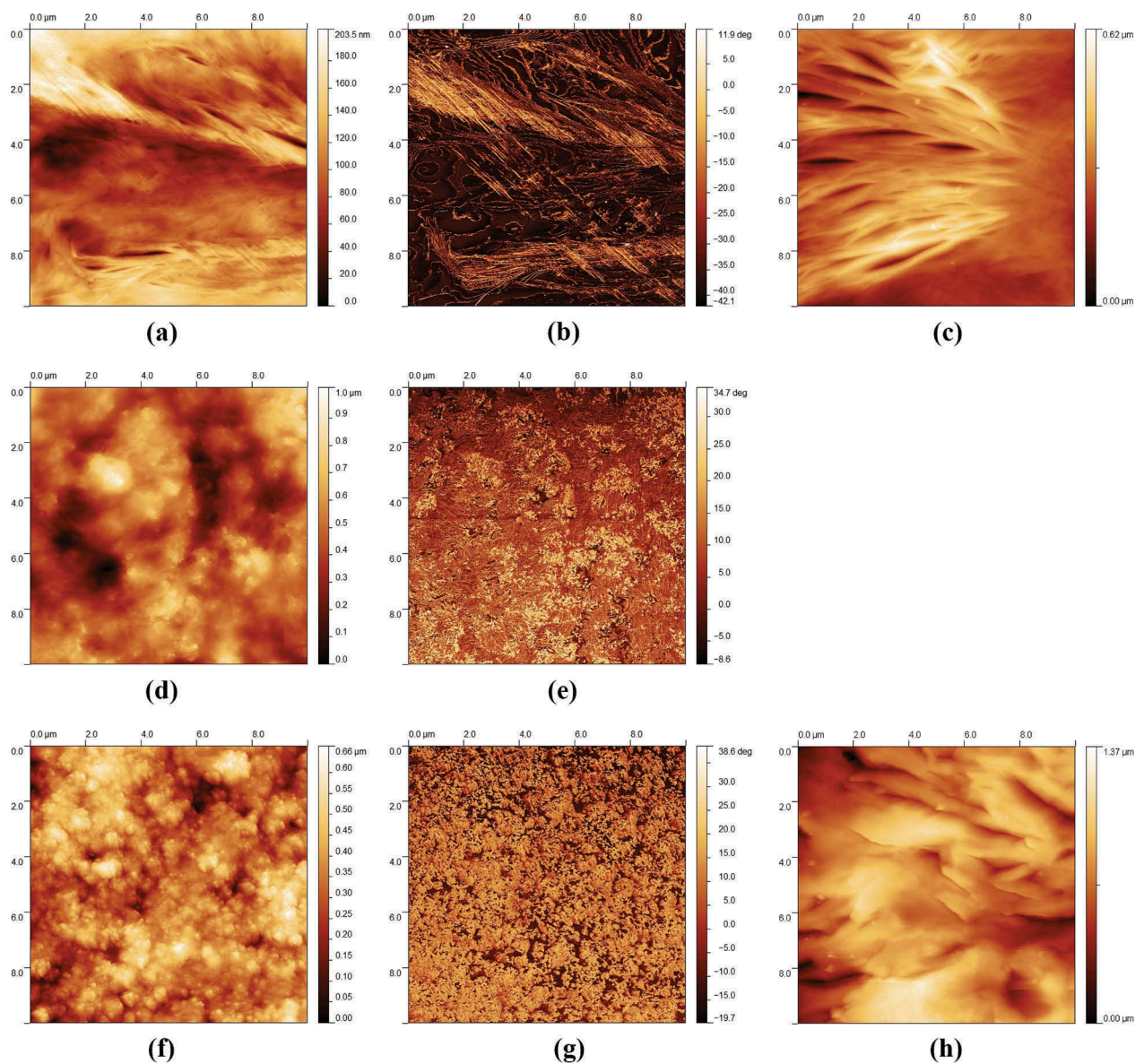


Figure 3. AFM images of (a) dry height (b) phase and (c) hydrated height of 0 wt.% nCHA composite coatings (d) dry height and (e) phase of 5 wt.% nCHA composite coatings (f) dry height (g) phase and (h) hydrated height of 10 wt.% nCHA composite coatings. Note: the colour scale on the images is not consistent.

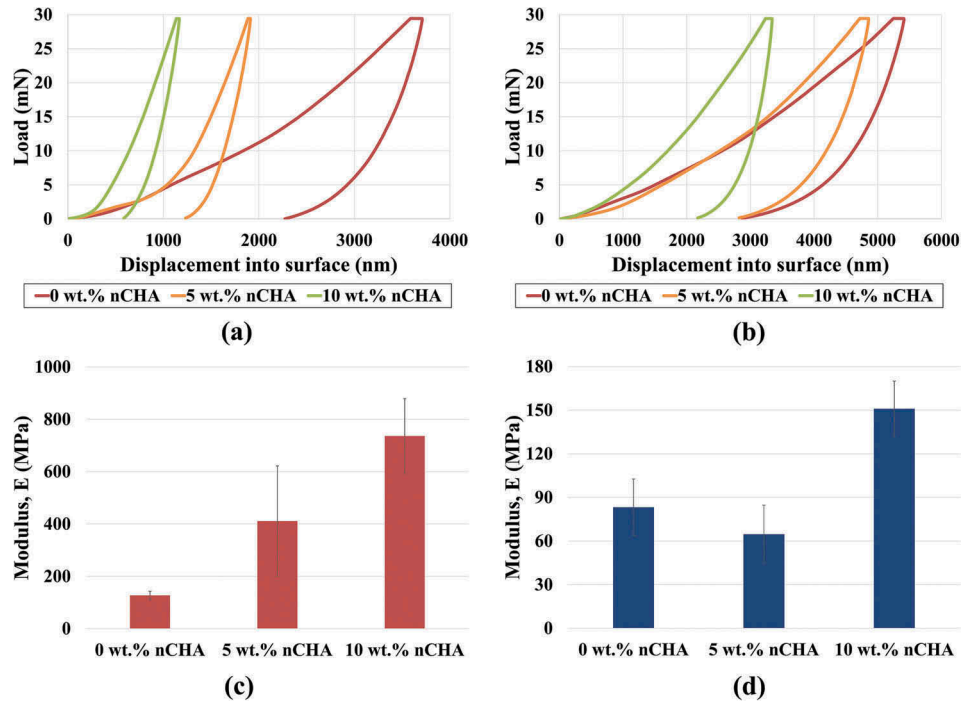


Figure 4. Load-displacement curves of PHEMA/PCL-nCHA composite coatings in (a) dry and (b) wet conditions, the modulus evaluated for the composite coatings in (c) dry and (d) wet conditions.

near-linear increase in modulus was noted with increasing filler content in wet conditions the 10 wt.% nCHA-containing sample clearly exhibited a higher modulus than the others (Figure 4(d)).

Figure 5 shows SEM micrographs of HOB cells on composite coating surfaces after 3 and 14 days in cell culture. After 3 days, HOB cells on the filler-free composite coating were observed to be spindle-shaped in morphology while flat- and irregular-shaped cells were observed for nCHA-containing composite coatings. After 14 days in culture, the cells on the filler-free composite coating showed

improved spreading and were similar in morphology to those on nCHA-containing composite coatings at day 3. The edge of the cell cytoplasm could not be easily distinguished. The morphology of HOB cells on 5 wt.% nCHA-containing composite coating surface changed very little from day 3 to day 14, maintaining the very flat- and irregular shape. However, the cytoplasmic edge of the flat cells on the 10 wt.% nCHA-containing composite coating surface appeared to be more distinguishable at day 14 than at day 3 and many filopodia were observed with evidence of extracellular matrix expression. In

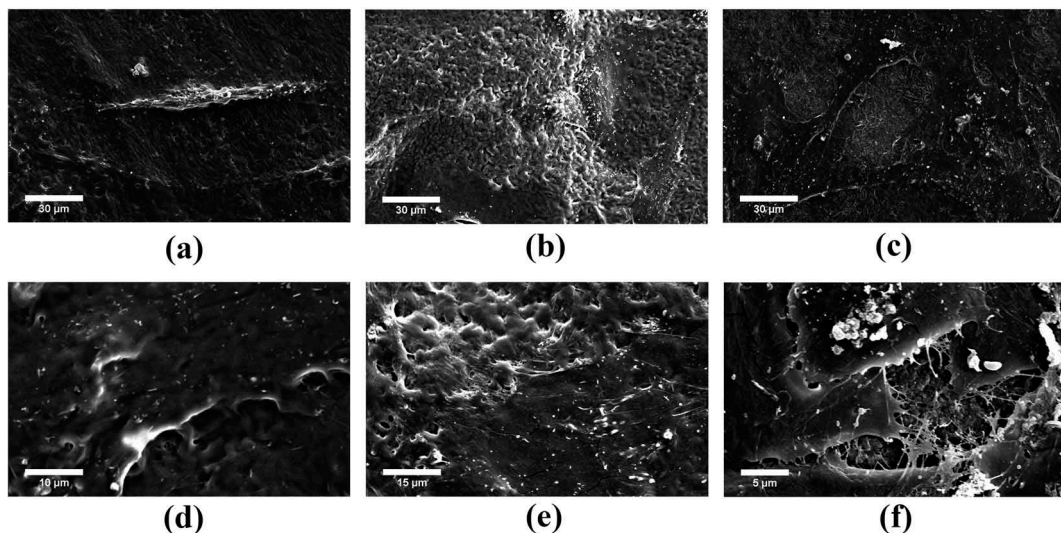


Figure 5. SEM micrographs of primary human osteoblast (HOB) cells on PHEMA/PCL-nCHA composite coating surface with (a) 0 wt.% nCHA (b) 5 wt.% nCHA and (c) 10 wt.% nCHA after 3 days in cell culture, (d) 0 wt.% nCHA (e) 5 wt.% nCHA and (f) 10 wt.% nCHA after 14 days in cell culture.

addition, globular precipitates with approximately 1–3 μm in diameter were observed on 10 wt.% nCHA-containing sample (Figure 5(f)). Point SEM-EDS analysis indicated that these precipitates were mainly composed of calcium and phosphorus (data not presented). The filler-free composite coatings were found to be partially peeled off the substrate by day 14 while the nCHA-containing composite coatings were still intact.

Discussion

A series of PHEMA-based nanocomposites were prepared as potential coating materials for metal implants.

A phase-pure nCHA was successfully produced in this study, containing about 4 wt.% carbonate, which is within the reported range for natural bone mineral [3]. In addition, all the peaks identified for carbonate group in the FTIR spectrum indicate that a mixed AB-type nCHA was produced [14,15].

The PHEMA/PCL-nCHA composites with varying filler weight fractions were coated on HCl-treated Ti-6Al-4V substrates. Well-attached and crack-free composite coatings were produced for filler contents up to 10 wt.% (Figure 2).

Both the surface morphology and filler distribution of the composite coatings were obtained from AFM analysis (Figure 3). Each of the bright particles observed in phase images of the filler-containing composite coating surfaces is very likely to be the representative of the nano-sized filler because of 2–3 orders of magnitude different modulus between the bioceramic filler and hydrogel polymer matrix. In addition, the shape and size of each particle agree well with the morphology of synthesised nCHA particles found by TEM (Figure 1(c)). The phase images of composite coatings reveal that the filler particles were dispersed patchily for 5 wt.%-containing composite coating while they were dispersed as a whole rather than region by region for 10 wt.%-containing composite coating. This dispersion of nCHA particles throughout the whole scanned area might be interpreted as showing that the PHEMA/PCL polymer matrix is only able to take up to 10 wt.% of the filler in the composite coating. Furthermore, some nCHA agglomerations could be seen together with discrete nCHA on the 10 wt.% nCHA composite coating surface. This might be why the composite coatings could not have been made with a higher filler content, without cracking.

The hydration response of 10 wt.% nCHA-containing composite coating was significant since the globules seen in dry state had completely disappeared after immersing the sample in DIW for 3 days. During the immersion period, the hydrogel, PHEMA in the composite system would have swollen, burying

both the nCHA particles and hydrophobic polymer PCL underneath the surface. The same swelling reaction would have occurred to the filler-free composite coating in wet conditions, explaining why the topographical features were similar regardless of the filler incorporation in the hydrogel polymer matrix.

The mechanical stability of coating was characterised using nanoindentation, which was performed in both dry and wet environments. Considering that the maximum indentation depth measured in all the tests, in both dry and wet environments, was kept to less than 10% of the coating thickness, $62.6 \pm 4.07 \mu\text{m}$ (not shown here), the substrate influence should have been minimised by the ‘rule of thumb’ [16]. Hence, the technique would have provided reasonably accurate modulus values of the composite coatings. In dry conditions, increasing the filler content produced a near-linear increase in modulus. However, no similar increase was noted with increasing filler content in wet conditions. This may be due to the presence and the mobility of water absorbed by the hydrogel polymer. During the loading period, the concentrated stress around the indenter would have allowed some of the water to be forced out near the indentation region together with the nCHA particles present in the composite systems. This might explain why the 5 wt.% nCHA-containing composite coating had a similar modulus to the filler-free coating sample.

The cellular response of human osteoblast (HOB) cells to PHEMA/PCL-nCHA composite coatings was assessed. The inclusion of nCHA particles in the hydrogel polymer matrix was shown to be beneficial since not only did it inhibit coating delamination during 14 days of incubation in culture medium but also improved the bioactivity of the composite coatings. When the coated sample is immersed in culture medium the medium would diffuse through the coating surface, rapidly hydrating the coating material, PHEMA. The medium would eventually reach the coating-substrate interface and consequently weakens the coating adhesion to its underlying substrate. However, the presence of nCHA particles at the interface would have improved the mechanical adhesion of the coating to the substrate compared to filler-free coatings, resulting in the greater stability of those coatings in wet environments. The observation of mineralised extracellular matrix on the 10 wt.% nCHA-containing composite coating after 14 days in culture has promising implications for the possibility of earlier bone-bonding *in vivo*. This preliminary study may warrant future investigation to obtain more evidence regarding the cellular response and the relative bioactivity of different types of the composite materials.

Overall, the hydrogel-nCHA composite coating containing 10 wt.% nCHA was shown to have the greatest coating stability and adhesion strength on Ti-

6Al-4V substrates both in wet and dry conditions. It also had the greatest bioactivity. Therefore, PHEMA/PCL with 10 wt.% nCHA appears to be the most promising coating material for metal implants such as bone plates and dental posts, which would not require a great insertion torque such as that needed for bone screws. This composite coating could provide a soft, low modulus interface between the metal implant and bone tissue, thereby reducing the stress shielding effect while encouraging the highest bioactivity compared with the other composites.

Acknowledgments

This work was supported by the Engineering and Physical Sciences Research Council (EPSRC). Dr. Roger Brooks acknowledges funding from the National Institute for Health Research. The raw data used to prepare for Figures 1 and 4 are available at the link: <https://doi.org/10.17863/CAM.22807>.

Disclosure statement

No potential conflict of interest was reported by the authors.

References

- [1] Van Noort R. Review titanium: the implant material of today. *J Mater Sci.* 1987;22:3801–3811.
- [2] Liu X, Chu PK, Ding C. Surface modification of titanium, titanium alloys, and related materials for biomedical applications. *Mater Sci Eng R Rep.* 2004;47:49–121.
- [3] Mkukuma LD, Skakle JMS, Gibson IR, et al. Effect of the proportion of organic material in bone on thermal decomposition of bone mineral: an investigation of a variety of bones from different species using thermogravimetric analysis coupled to mass spectrometry, high-temperature X-ray diffraction, and Fourier transform infrared spectroscopy. *Calcif Tissue Int.* 2004;75:321–328.
- [4] Landi E, Celotti G, Logroscino G, et al. Carbonated hydroxyapatite as bone substitute. *J Eur Ceramics Soc.* 2003;23:2931–2937.
- [5] Porter A, Patel N, Brooks R, et al. Effect of carbonate substitution on the ultrastructural characteristics of hydroxyapatite implants. *J Mater Sci: Mater Med.* 2005;16:899–907.
- [6] Hasegawa M, Doi Y, Uchida A. Cell-mediated bioresorption of sintered carbonate apatite in rabbits. *J Bone Joint Surg Br.* 2003;85-B:142–147.
- [7] Netti PA, Shelton JC, Revell PA, et al. Hydrogels as an interface between bone and implant. *Biomaterials.* 1993;14:1098–1104.
- [8] Peluso G, Petillo O, Anderson JM, et al. The differential effects of poly(2-hydroxyethylmethacrylate) and poly(2-hydroxyethyl methacrylate)/poly(ϵ -caprolactone) polymers on cell proliferation and collagen synthesis by human lung fibroblasts. *J Biomed Mater Res.* 1997;34:327–336.
- [9] Lee S-Y, Regnault WF, Antonucci JM, et al. Effect of particle size of an amorphous calcium phosphate filler on the mechanical strength and ion release of polymeric composites. *J Biomed Mater Res B Appl Biomater.* 2007;80:11–17.
- [10] Roohani-Esfahani S-I, Nouri-Khorasani S, Lu Z, et al. The influence hydroxyapatite nanoparticle shape and size on the properties of biphasic calcium phosphate scaffolds coated with hydroxyapatite-PCL composites. *Biomaterials.* 2010;31:5498–5509.
- [11] Wilberforce SIJ, Finlayson CE, Best SM, et al. The influence of hydroxyapatite (HA) microparticles (m) and nanoparticles (n) on the thermal and dynamic mechanical properties of poly-L-lactide. *Polymer.* 2011;52:2883–2890.
- [12] Gibson IR, Bonfield W. Novel synthesis and characterization of an AB-type carbonate-substituted hydroxyapatite. *J Biomed Mater Res.* 2002;59:697–708.
- [13] Johnson KL. Contact mechanics. Cambridge, U.K.: Cambridge University Press; 1985.
- [14] Koutsopoulos S. Synthesis and characterization of hydroxyapatite crystals: a review study on the analytical methods. *J Biomed Mater Res.* 2002;62:600–612.
- [15] McConnell D. Chapter 7: carbonate apatites. New York: Springer-Verlag; 1973. ((Apatites: Its crystal chemistry, mineralogy, utilization, and geologic and biologic occurrences)).
- [16] Tsui TY, Pharr GM. Substrate effects on nanoindentation mechanical property measurement of soft films on hard substrates. *J Mater Res.* 1999;14:292–301.